## Supplemental figures

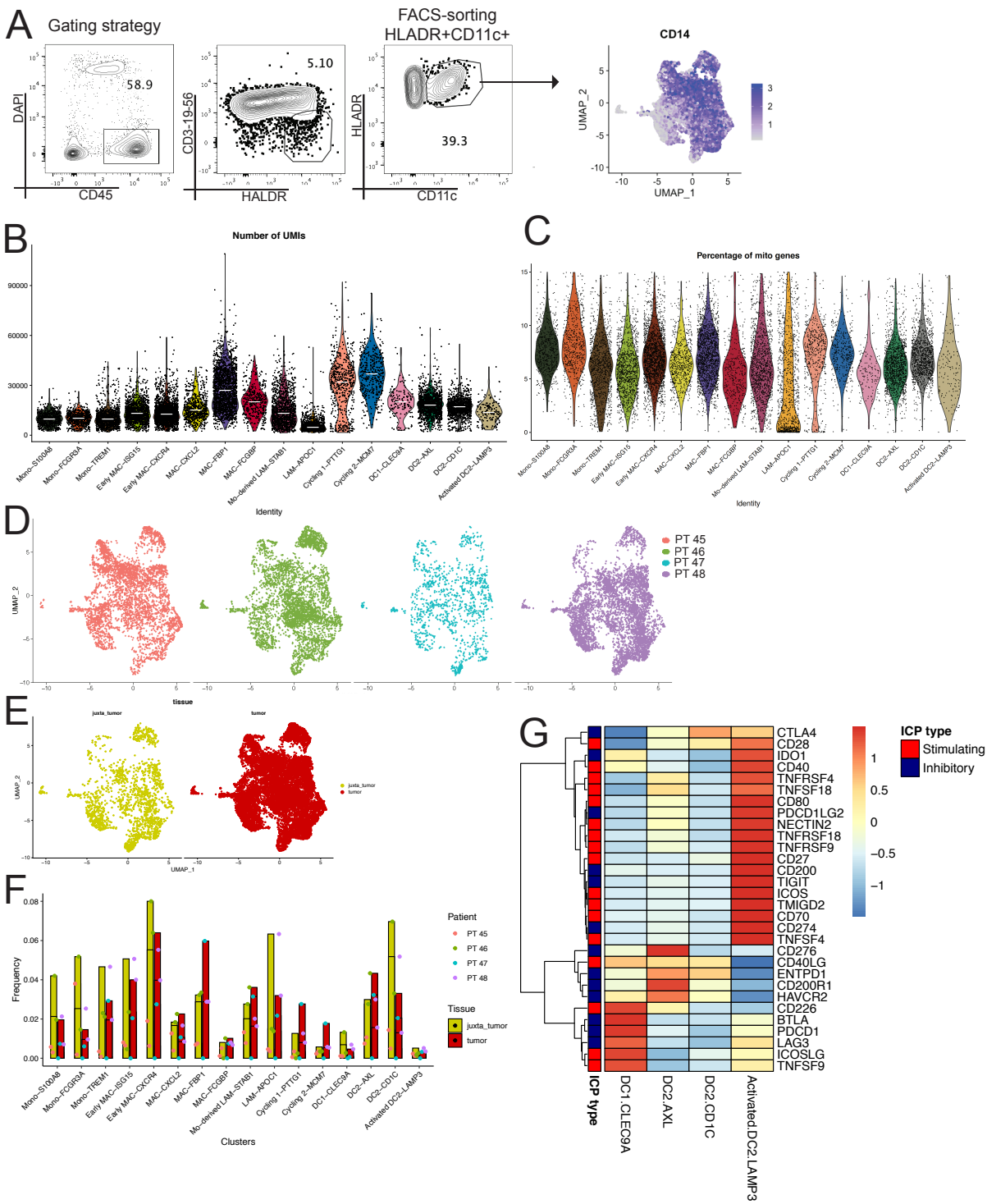


Suppl. Figure 1

**Figure Suppl. 1:** (A) Representative gating strategy for FACS-sorting of HLADR$^{+}$CD11c$^{+}$ myeloid cells for scRNAseq analysis, UMAP showing CD14 expression in merged JT and TUM samples (B-C) Violin plot of the number of unique molecular identifiers (UMI) and percentage of mitochondrial genes for each cluster in merged JT and TUM samples. (D) UMAP representation of 14134 myeloid cells representing patient by patient merged JT and TUM; (E) JT versus TUM all merged patients. (F) Box plot representing the average frequency of the 16 myeloid cell clusters from 4 TNBC pts in JT and TUM specimens. Means are shown. (G) Cluster-averaged heatmap of inhibitory and stimulatory checkpoints in merged (JT and TUM) DCs.

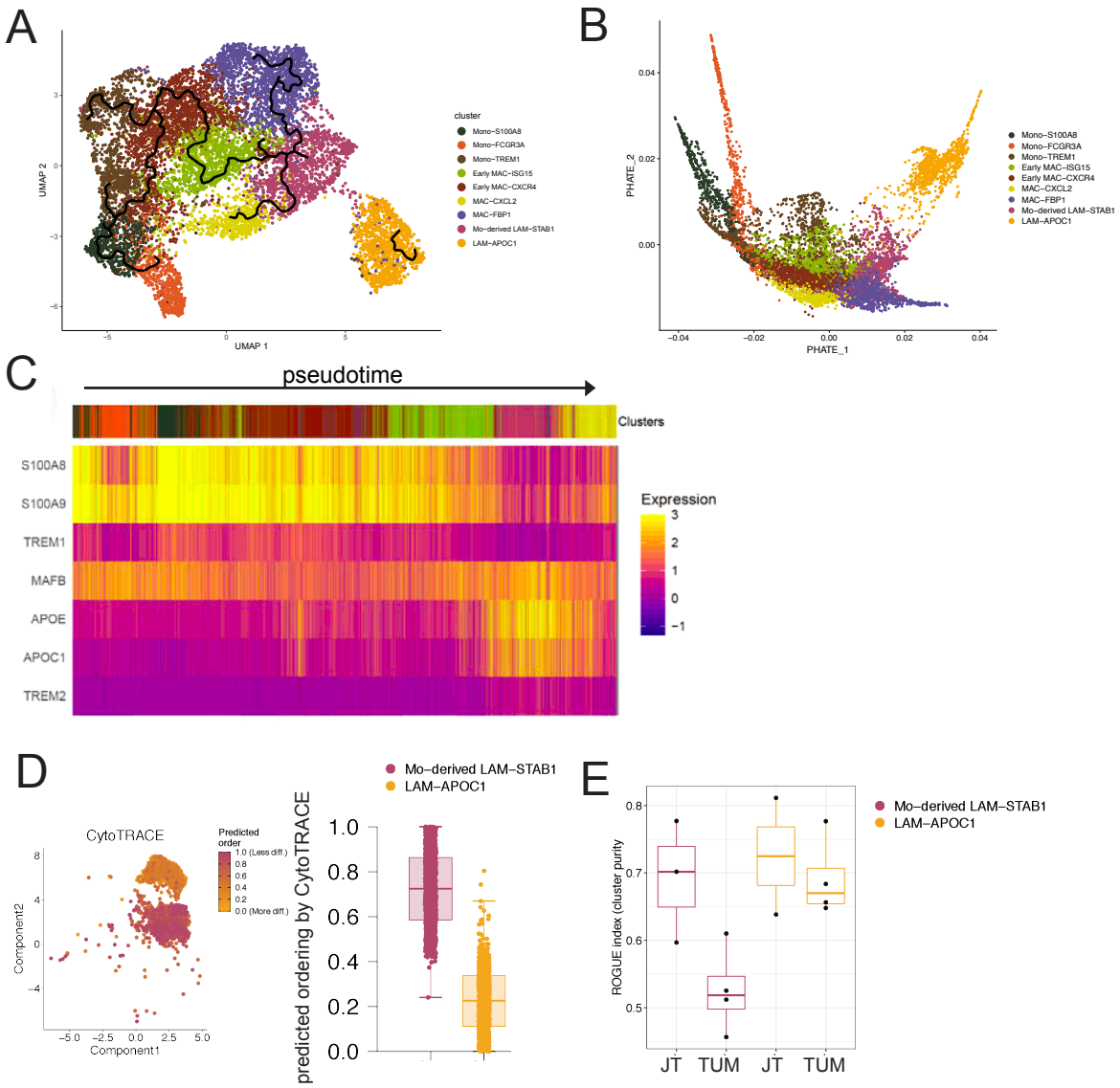


Suppl. Figure 2

**Figure Suppl. 2: LAMs comprise resident and monocyte-derived MAC**

(A-B) Trajectory inference analysis by Monocle and PHATE algorithm. (C) Pseudotime analysis of single genes (*S100A8, S100A9, TREM1, MAFB, APOE, APOC1, TREM2*), using the cell expressing the monocyte marker *S100A8* as cell of origin. (D) CytoTRACE algorithm showing mo-derived LAM-STAB1 and LAM-APOC1 in UMAP visualization (left panel), predicted CytoTRACE ordered values showed in total mo-derived LAM-STAB1 and LAM-APOC1 (right panel). (E) ROGUE index analysis of JT and TUM mo-derived LAM-STAB1 and LAM-APOC1 clusters.

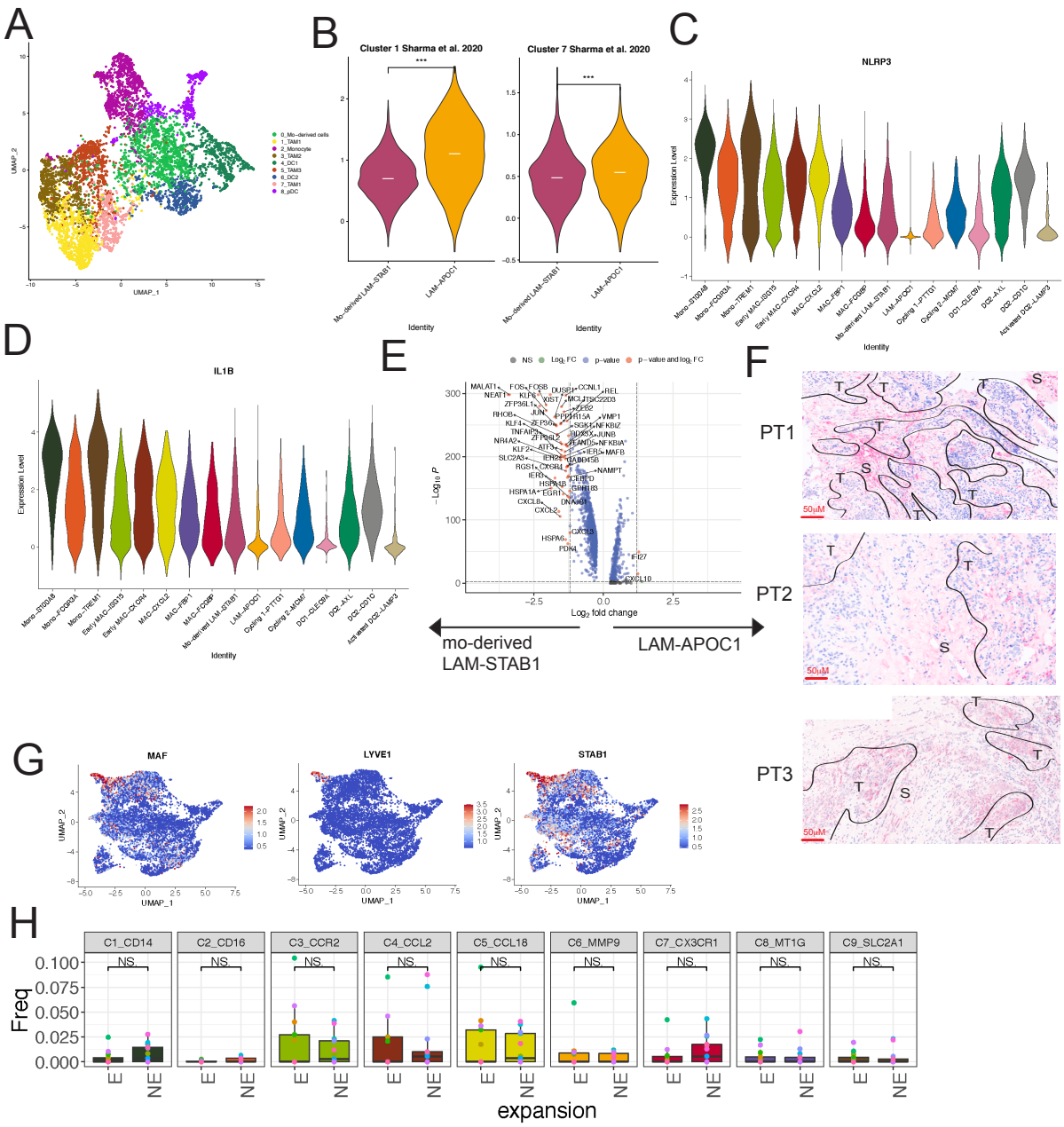


Suppl. Figure 3

**Figure Suppl. 3:** (A) UMAP representation of myeloid cells recomputed from Sharma et al. (15) (B) Violin plots of the cluster 1 (tissue-resident) and cluster 7 (reprogrammed monocyte-

derived) global signatures Sharma et al (15), projected in the total mo-derived-LAM-STAB1 and LAM-APOC1 TNBC clusters; medians are shown in white, *** $p < 0.001$ by Unpaired t-test. (C-D) Violin Plots of NLRP3 and IL1B in each cluster of merged JT and TUM samples. (E) Volcano plot showing DEGs of total mo-derived-LAM-STAB1 *vs* LAM-APOC1 cluster. Wilcoxon test. (F) H&E staining are shown in 3 representative treatment-naïve TNBC samples, referring to the Figure 3J. Black lines indicate T: tumor and S: stroma areas in the tumor sections.

(G) Expression of MAF, FOLR2, LYVE1 and STAB1 in the myeloid dataset from Bassez et al. (29). (H) Frequency of different annotated clusters from Bassez et al. (29) in E (expanded) *versus* NE (non-expanded) anti-PD1 treated TNBC patients.

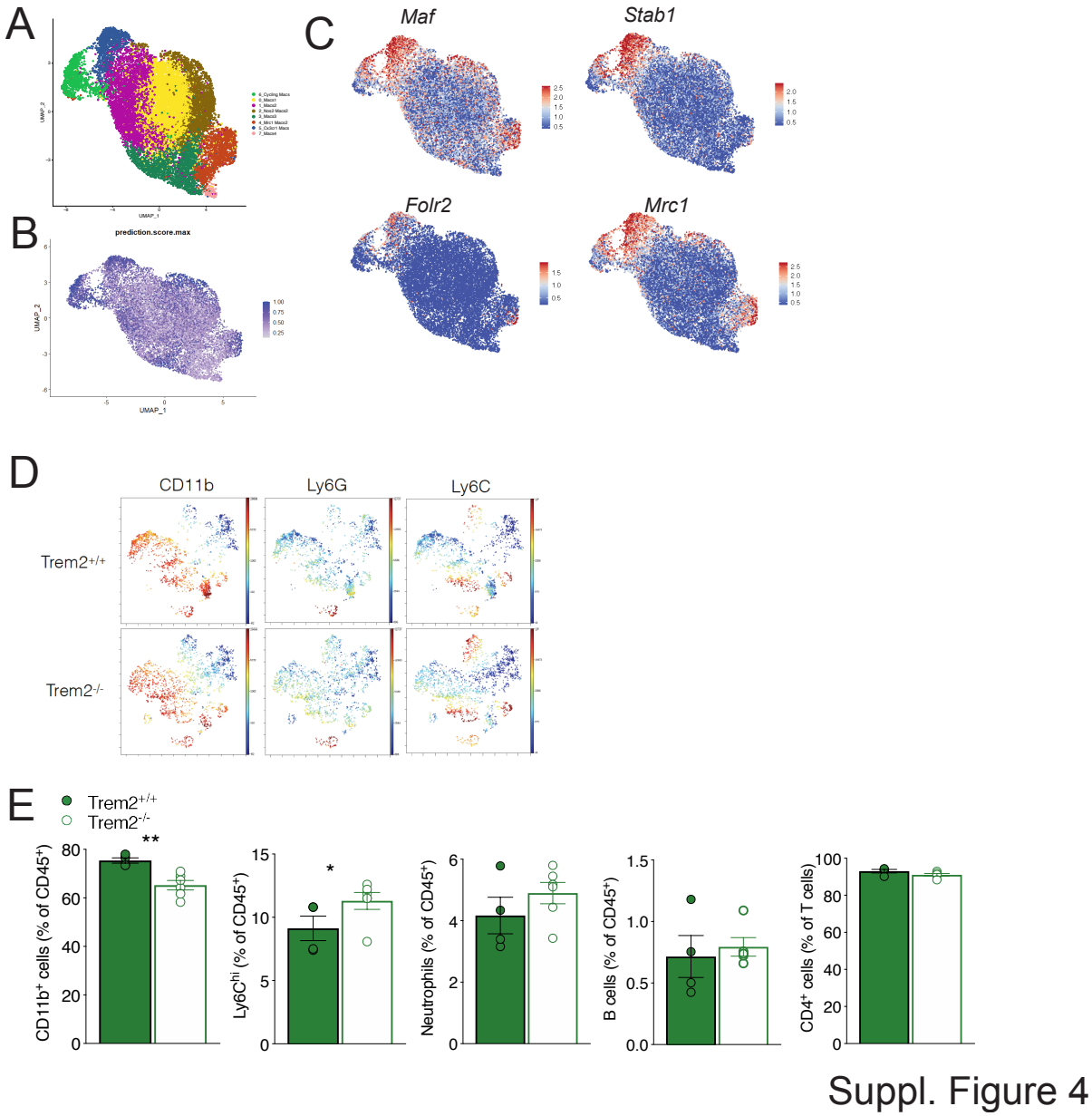


**Figure Suppl. 4:** (A) UMAP representation of myeloid cells recomputed from Molgora et al. (18) (B) UMAP representation of maximum prediction score for each cell after doing label transfer from our TNBC datasets into mouse sarcoma *Trem*2$^{+/+}$ and *Trem2*$^{-/-}$ merged datasets (18). (C) Expression of *Maf*, *Stab1*, *Folr2* and *Mrc1* in the mouse sarcoma *Trem*2$^{+/+}$ and *Trem2*$^{-/-}$ merged datasets (18). (D) t-SNE representation of one representative *Trem*2$^{+/+}$ and *Trem2*$^{-/-}$ tumor gated on CD45$^{+}$ showing CD11b, Ly6G and Ly6C expression. (E) Graphs showing tumor FC analysis of the percentage of CD11b$^{+}$, Ly6C$^{high}$, neutrophils (CD11b$^{+}$Ly6G$^{+}$), B cells gated on CD45$^{+}$ cells and CD4 T cells gated on total TCRβ$^{+}$ cells. * $p < 0.05$, ** $p < 0.01$ by Mann-Whitney t-test.

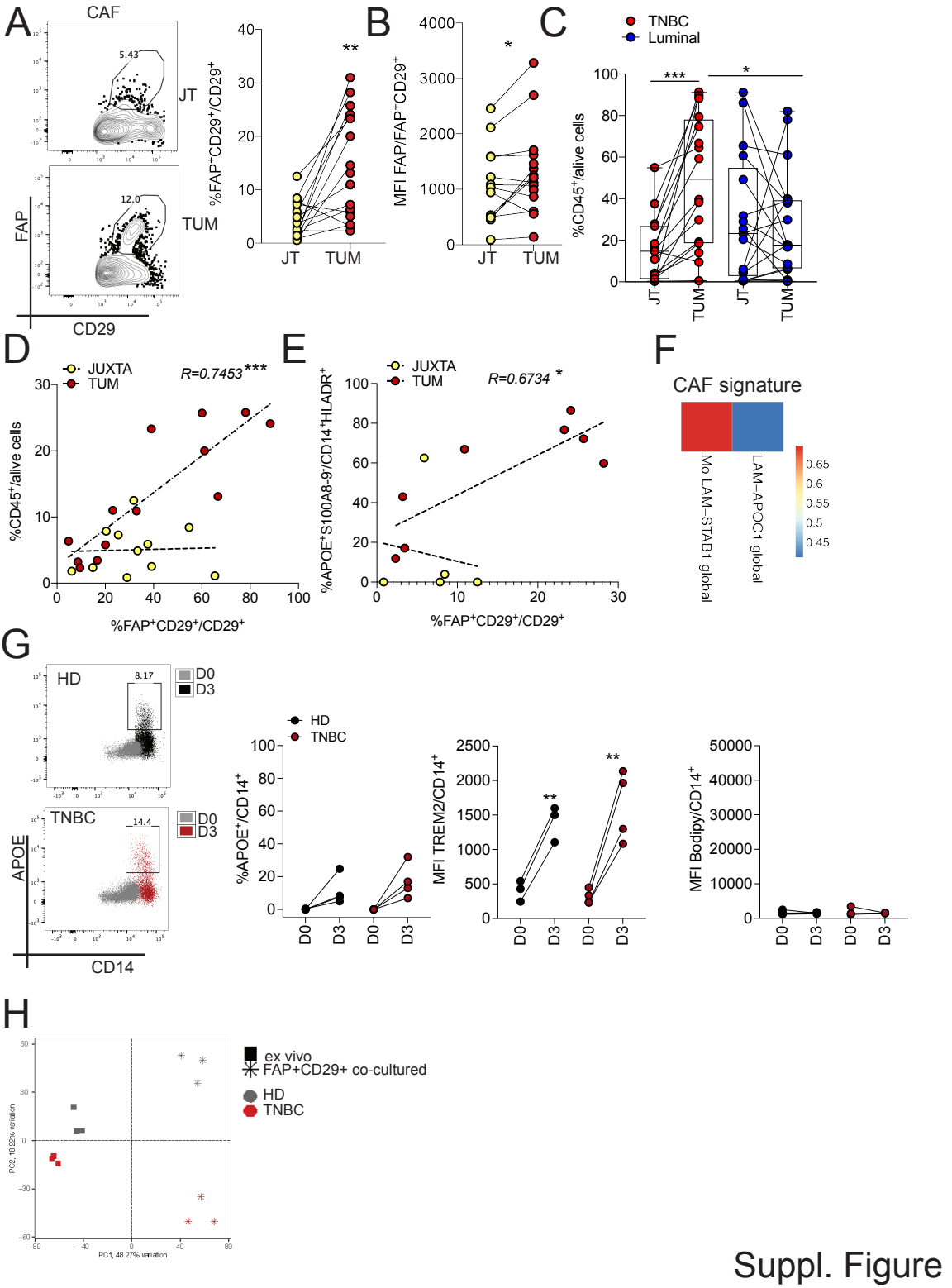


Suppl. Figure 5

**Figure Suppl. 5:** (A) Representative FAP/CD29 FC staining (left panel) and percentages (right panel) of $FAP^+CD29^+$ cells in live $CD29^+CD31^-CD235a^-CD45^-$Epcam- CAF cells in JT and TUM (N=14; TNBC =7, LBC N=7; ** $p < 0.01$ by Paired t-test, two-tailed). (B) FAP MFI by FC in $FAP^+CD29^+$ gated cells in JT and TUM (N=14; TNBC =7, LBC N=7; * $p < 0.05$ by Paired t-test, two-tailed). (C) Percentage of $CD45^+$ cells gated on live cells, analyzed by FC, in JT and TUM of TNBC (N=16) and LBC (N=17) pts. (D) Pearson correlation between the percentage of $CD45^+$ and $FAP^+CD29^+$ cells in all cohorts (TNBC *plus* LBC), JT (N=11) and TUM (N=13). *** $p < 0.001$. (E) Pearson correlation between the percentage of $APOE^+S100A8\text{-}9^-$ and $FAP^+CD29^+$ cells in JT (N=5) and TUM (N=8). * $p < 0.05$. (F) Heatmap showing Spearman correlation between the signatures of CAF ($FAP^+CD29^+$) *vs* mo-derived-LAM-STAB1 and LAM-APOC1 clusters by bulk RNA-analysis in the METABRIC TNBC cohort (N=332). (G) FC analysis of HD- (N=4) and TNBC-derived (N=4), magnetically enriched blood monocytes, before (day 0) and after (day 3) CAF-circulating monocyte cocultures *in vitro*. Both $FAP^+CD29^+$ and $FAP^-CD29^+$ primary CAF cell lines were derived from primary TNBC tissues (Figure 5A-B-C). (G-left panels) Representative APOE/CD14 FC staining and percentages of $APOE^+$ cells in $CD14^+$ gated cells, at day 0 and 3 from $FAP^-CD29^+$ CAF-monocyte co-culture. (G-middle, right panel) MFI of TREM2 and Bodipy by FC in $CD14^+$ gated cells at day 0 and 3 from $FAP^-CD29^+$ CAF-monocyte co-culture. ** $p < 0.01$ by Paired t-test, two-tailed. (H) Principal component Analysis (PCA) plot on the variance stabilized data from DESeq2. PC1: co-culture conditions (*ex vivo* and $FAP^+CD29^+$-cocultured) and PC2: origin of monocytes (HD and TNBC).

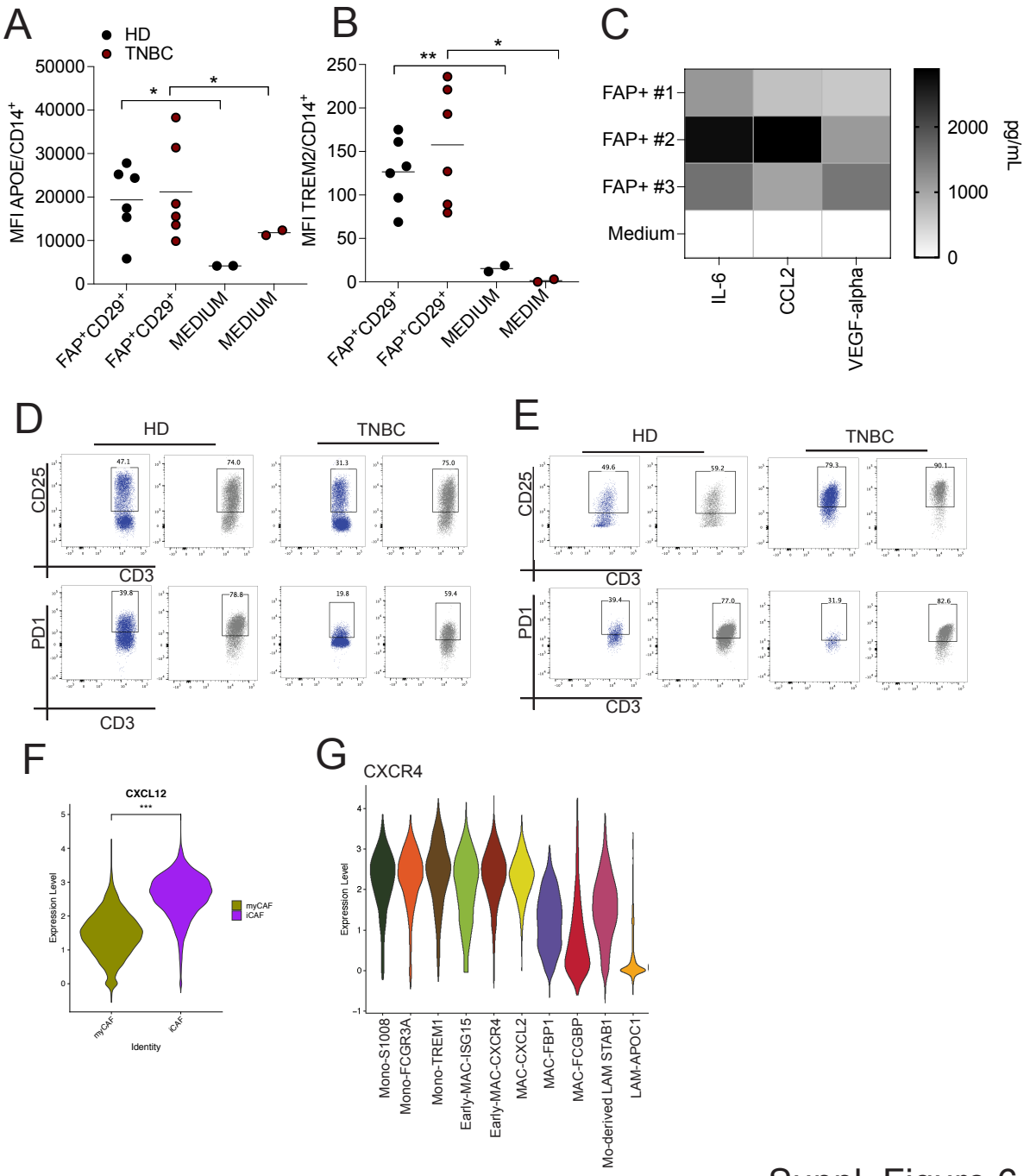


Suppl. Figure 6

**Figure Suppl. 6**: (A-B) Freshly isolated CD14+ monocytes from HD and TNBC were co-cultured for 3 days with FAP$^{+}$CD29$^{+}$- supernatants. MFI of APOE and TREM2 in CD14$^{+}$

monocytes is evaluated by FC analysis at day 3 in $FAP^+CD29^+$- supernatant and control (medium) conditions. Three $FAP^+CD29^+$ cell lines were used to generate supernatants. Three pooled independent experiments in duplicates are shown. * $p < 0.05$, ** $p < 0.01$ by Unpaired t-test, two-tailed. (C) Cytokines/chemokines were evaluated in $FAP^+CD29^+$ supernatants, generated from three different CAF cell lines (FAP+ #1, FAP+ #2, FAP+ #3) by Human Procarta-Plex Immunoassay. Heat Map show IL-6, CCL2 and VEGF-α data as pg/mL. The experiment has been done in duplicates. (D-E) CD14+-Miltenyi enriched monocytes from HD (N=4) and TNBC (N=4) were co-cultured with $FAP^+CD29^+$ and $FAP^-CD29^+$ CAF for 3 days (Figure 6B-C). Mo-derived-LAM were then co-cultured with autologous, CFSE labelled $CD3^+$ T cells. At day 3, $CD4^+$ and $CD8^+$ T cells from both HD and TNBC were assessed for PD1 and CD25 expression. Representative FC plots of CD25/CD3 and PD1/CD3 staining gated on CD4 T cells (D) and CD8 T cells (E). (F) Violin plot of CXCL12 expression in iCAF and myCAF clusters. *** $p < 0.001$ by Unpaired t-test. (G) Violin Plot of CXCR4 expression on myeloid clusters.